

OPTICS IMPROVEMENTS OF THE K500 AXIAL INJECTION LINE

M. Doleans, S. Chouhan, D. Cole, G. Machicoane, F. Marti, P. Miller, J. Moskalik, M. Steiner, J. Stetson, X. Wu, P. Zavodszky, A. Zeller, Q. Zhao, NSCL/MSU, East Lansing, MI 48824, U.S.A.

Abstract

Recent improvements in the K500 injection beam line optics have increased the injection efficiency into the K500 cyclotron and lead to record primary beam powers on the production target at the CCF (Coupled Cyclotron Facility). For example, consecutive improvements in the design of the electrostatic focusing system below the ECR ion source have gradually increased the beam brightness. Also, degradation of the beam brightness by field aberrations in the existing analyzing bending magnets has been identified and remedied. During this effort, the offline ECR source Artemis-B has been a key factor allowing in-depth R&D without reducing beam time for the CCF operation. In the beam studies, emphasis has been put toward systematic quantification of the beam brightness using Allison-type emittance scanners. Various improvements in the K500 injection beam line optics will be presented and discussed.

REVIEW OF INJECTION BEAMLINE IMPROVEMENTS

In the last three years, a sustained R&D effort has been carried at the NSCL to improve the beam brightness in the CCF injection beam line. For example, a new superconducting ECR ion source, SuSI [1,2], has been built to replace the existing SC ECR ion source and to increase the primary beam power for heavy ions. Early beam commissioning results of SuSI are discussed in [3]. In parallel, Artemis-B [4], an offline replica of the 14 GHz RT (Room Temperature) ECR source Artemis was built in 2005 and extensively used since for ion source and beam optics development. Artemis-B test stand has also been very valuable for the commissioning of new hardware prior to its installation in the injection beam line of the CCF. A current layout of the injection beamline is shown in Figure 1.

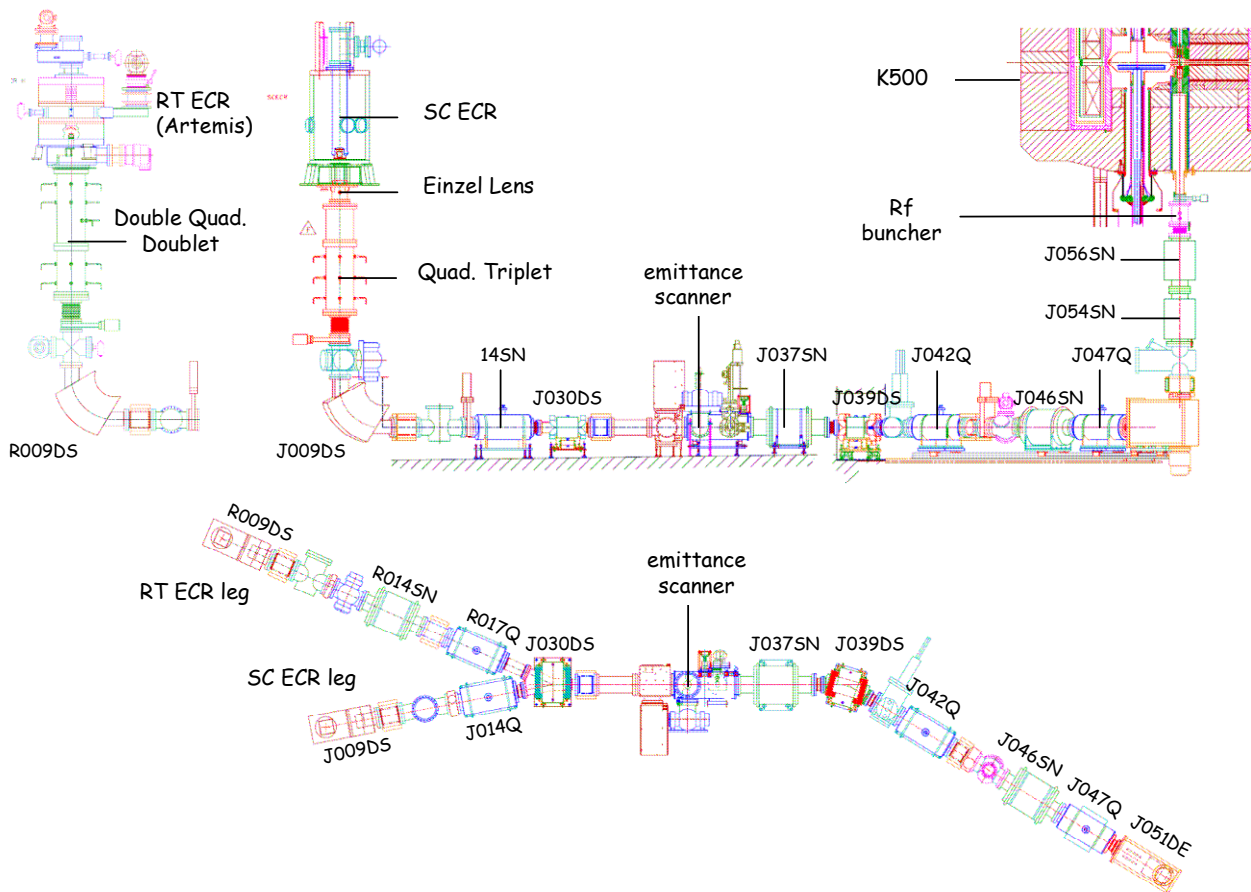


Figure 1: Layout of the CCF beam injection line. Side view of RT ECR (upper left), side view of SC ECR and injection line (upper right) and top view of injection line (bottom). Magnetic focusing solenoids were replaced by electrostatic focusing systems under both ECR sources to avoid possible space charge effects. After the charge state selection, magnetic and electrostatic elements are used for focusing.

Recent Hardware development included:

- Allison-type emittance scanner
- Electrostatic focusing elements before charge state selection
- New 90-degree analyzing magnets
- Horizontal and vertical movable slits system

On-going hardware development includes:

- Beam chopper
- Grid-less two-harmonics rf-buncher
- Electrostatic spherical bender

In addition to new hardware, swapping/addition of some beam line focusing elements were done to improve the beam matching into the K500 cyclotron. Finally, to help shortening the beam tuning time, automatic tuning software is being developed. In the next sections, developments related to the emittance scanner, to the electrostatic focusing elements below the ECR and to the new analyzing magnet will be detailed.

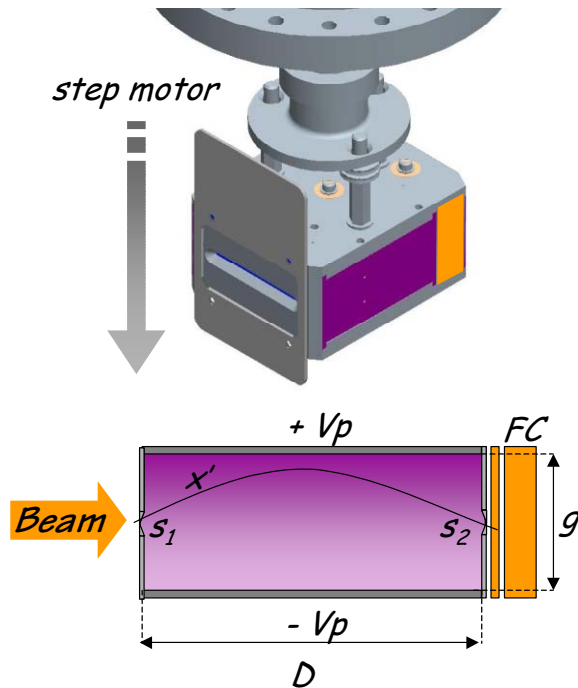


Figure 2: NSCL Allison-type emittance scanner. See text for details.

ALLISON EMITTANCE SCANNER

The systematic use of the emittance scanner during R&D work on Artemis-B has been a key factor in the improvement of the injection beam line optics. The design of the NSCL Allison emittance scanner and is based on a similar device operated at LBL [5]. As shown in Figure 2, the emittance scanner box has entry and exit slits (s_1 and s_2) of 60×0.5 mm size separated by a distance $D=75$ mm. Between the slits, two deflecting voltage plates ($\pm V_p$) are separated by a distance $g=12$ mm. After the second slit a Faraday Cup (FC) collects the beamlet currents. The emittance box is scanned across the beam using a step

motor and at each position the voltages on the plates are scanned to collect all possible beamlet angles. The relation between the voltage on a the plates and the angle is

$$V_p = \frac{2g}{D} V_{ECR} x'$$

where V_{ECR} is the ECR extraction voltage and for example, particles with $x'=50$ mrad extracted at $V_{ECR}=25$ kV need $V_p=400$ V to be collected in the Faraday cup of the emittance scanner box. After the emittance is measured, a brightness curve (i.e. beam current within emittance) is generated. Examples of emittance measurements and details about the emittance scanner software were presented in [6]. Various focusing elements were tested below Artemis-B and the beam brightness measured in each case. Particularly, the difference between magnetic focusing elements and electrostatic elements was investigated.

FOCUSING AFTER ECR: MAGNETIC VS ELECTROSTATIC

Basic scaling laws

Ion beams extracted from ECR have multiple charge states and possibly multiple species (e.g. when a support gas is used). These beams are nonrelativistic and the electrostatic and magnetic rigidities are given by

$$E\rho = 2V_{ECR}$$

$$B\rho = \sqrt{\frac{2m_0}{e}} \frac{A}{Q} V_{ECR}$$

with m_0 the atomic mass unit and e the elementary charge and with A/Q the mass to charge ratio of the considered ion. For convenience, the second equation can be rewritten

$$B\rho [T \cdot m] \approx 4.554 \times 10^{-3} \sqrt{\frac{A}{Q} V_{ECR} [kV]}$$

For example, a $^{40}\text{Ar}^{7+}$ beam extracted at 25 kV from the ECR has $B\rho \sim 0.0544$ T·m. As shown in [7], below $\beta \sim 1.7 \times 10^{-2}$ electrostatic focusing devices are more efficient than magnetic elements. At the CCF, beams injected into the K500 cyclotron have typical velocities $\beta \sim 0.003$ and magnetic and electrostatic focusing options are almost equally efficient. Nonetheless, the previous equations show that the electrostatic rigidity is independent of the mass and charge of the ion whereas the magnetic rigidity scales with the square root of their ratio. As explained in the next section, this difference makes the magnetic option more susceptible to beam brightness degradation from space charge effects.

Space charge effects for magnetic focusing

At the CCF, focusing solenoids were originally used as focusing elements between the ECR ion sources and the analyzing magnets. In some cases, images of the beam on

viewer plates of the K500 injection line appeared hollow [8]. This observation was attributed to the effect of space charge forces from ions with higher Q/A than the ion of interest [9]. To avoid such problems it was proposed to replace the magnetic focusing solenoids with electrostatic focusing elements. Beam simulations using a Particle-In-Cell code were performed to estimate the possible gain in beam brightness [10]. Though hollow beams were observed, the degradation of the beam emittance caused by the space charge forces wasn't quantified experimentally. Such a beam study was recently conducted on Artemis B and detailed results can be found in [11]. The main results from this study are reproduced below.

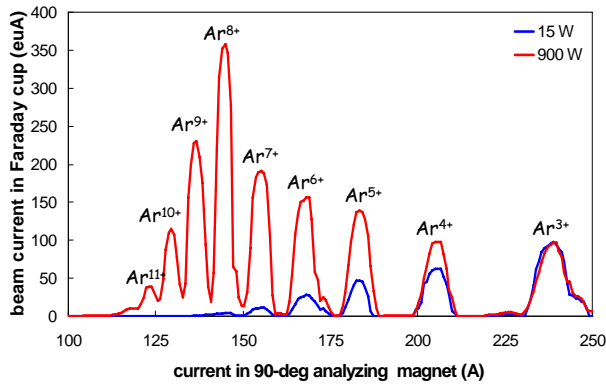


Figure 3: Charge State Distribution (CSD) for Argon beam measured on Artemis-B for 15 W and 900 W of rf microwave power injected into the ECR plasma.

In the measurements, an Argon beam was produced by the Artemis-B ion source without support gas and extracted at 20kV. The source was kept in the same conditions throughout the measurements and only the microwave power level was changed. In a first case, the source was run with only 15 W of microwave power. In a second case, the source was run at 900 W. The CSD (Charge State Distribution) for these two cases is shown in Figure 3. The total beam current extracted from the source was 0.5 mA and 2 mA for the low and high power case respectively. In both measurements, the transmission efficiency from the ECR to the faraday cup after the analyzing magnet was 80%. In the 900 W case, the proportion of higher charge state ion (i.e. $Q > 7+$) is dramatically increased compared to the 15 W case. This is the most important difference between the two cases since space charge effects from higher Q/A ions on lower Q/A ions is the main cause of beam brightness degradation.

Pictures for the different charge states of the Argon beam were recorded on a beam viewer located one meter after the Faraday cup and are shown in Figure 4 for the low power case and in Figure 5 for the high power case. To obtain the pictures, the magnetic fields in the focusing solenoid and in the analyzing magnet were successively adjusted according to the magnetic rigidity of each particular charge state.

Deformations on the outside edge of the beam can be observed on every pictures. This effect is due to the focusing solenoid leads, which run parallel to the beam axis for a few centimeters and generate azimuthal magnetic field components. The azimuthal components interact with the axial velocity of the ions and lead to radial aberrations [12].

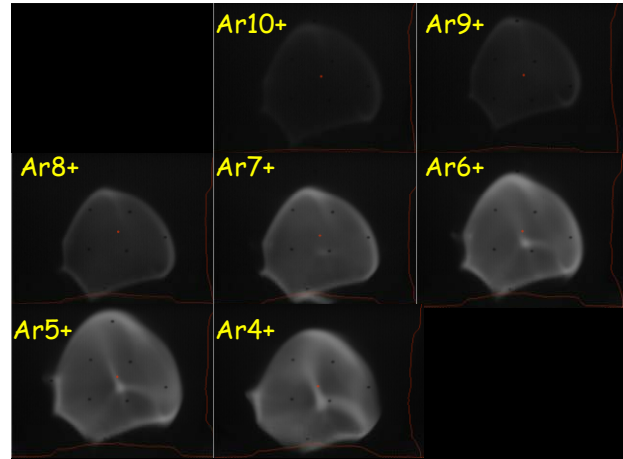


Figure 4: Pictures of the different charge states of an Argon beam on a beam viewer located one meter after the analyzing magnet for the 15 W case.

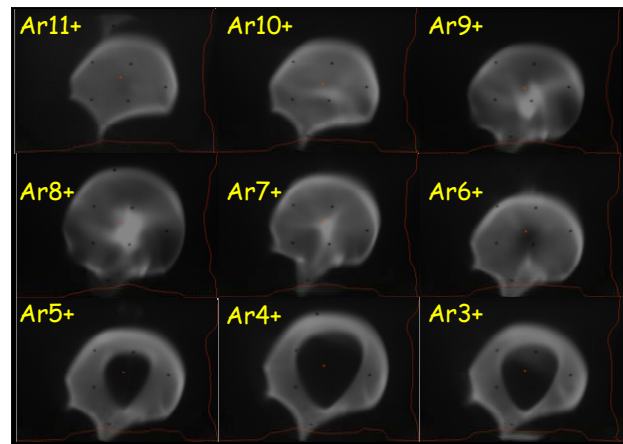


Figure 5: Same as Figure 4 but for the 900 W case.

The beam pictures for the 15 W and 900 W are significantly different. For the lower power case, all the charge state pictures have similar features beside for the difference in overall intensity and for some finer details that are not yet understood (e.g. bright spots in the middle). For the higher power case, the difference between the pictures of the different charge states is much more pronounced with the lower charge states (i.e. $Q < 6+$) having hollow distributions. The significant difference between the low and high power measurements is consistent with effects from space charge forces. In the low power case, the beam current for all the charge states is small and space charge forces are negligible. In the high power case, the higher Q/A beams produce significant

repulsive forces on the core part of the lower Q/A beams that lead to hollow beam distributions.

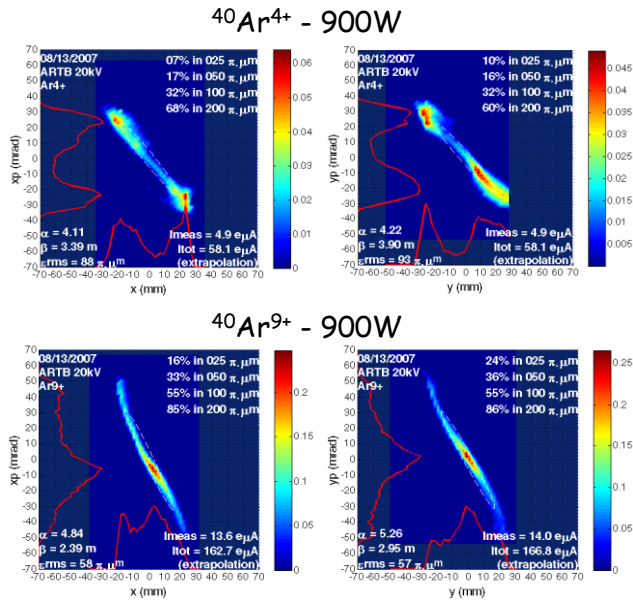


Figure 6: Transverse emittances for Ar^{4+} and Ar^{9+} beams for the 900 W case. The Ar^{4+} emittances are hollow while the Ar^{9+} emittances are centered on a core. For the 15 W case no hollow emittances could be observed.

Further characterization was done for Ar^{4+} up to Ar^{9+} by measuring the horizontal (xx') and vertical (yy') beam emittances in the Allison emittance scanner. The scanner was located 2.5 m after the analyzing magnet and a solenoid was used in between to refocus the beam. The measured emittances for Ar^{4+} and Ar^{9+} in the high power case are shown in Figure 6. The phase space distributions for Ar^{9+} are centered on intense cores while the distributions for Ar^{4+} appear hollow. This result is in qualitative agreement with the pictures observed on the beam viewers upstream.

The percentage of beam included within a given emittance for Ar^{5+} for the two different cases of microwave power are plotted in Figure 7. The emittance of Ar^{5+} has degraded significantly as the microwave power was increased, going from 60 % of beam included within $100 \pi \mu\text{m}$ for the case at 15 W to about 30 % for the case at 900 W.

The experimental results collected on Artemis-B are consistent with the beam brightness degradation by space charge forces. In the low space charge regime, the focusing solenoid is an efficient focusing element. In the high space charge regime, using a solenoid can lead to significant beam emittance degradation. Because space charge effects were found to be a problem for some beams at the NSCL, development of electrostatic focusing systems below the ECRs was pursued.

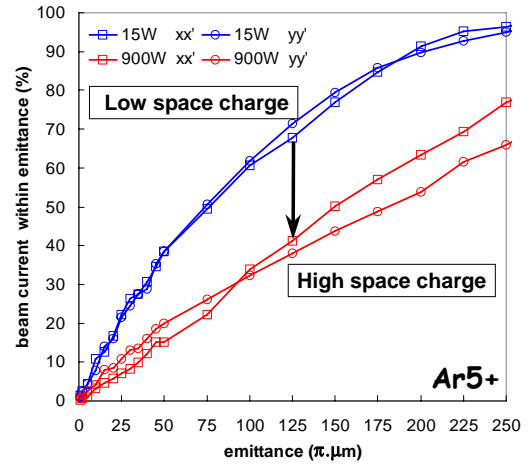


Figure 7: Transverse beam emittances for Ar^{5+} beam and for the two different cases of microwave power. For the low power case, the space charge forces are small and have a negligible effect on the beam brightness. In the high power case, the space charge forces are significant and the brightness is degraded.

Electrostatic focusing system design

The first electrostatic system designed and installed at the NSCL was a small bore electrostatic quadrupole triplet. Because of its modest three-inch aperture, the beam transmission efficiency from the ECR to the analyzing magnet was poor ($\sim 25\%$ compared to $\sim 80\%$ for the solenoid) but encouraging results were nonetheless achieved in the CCF using this device [8]. The limitation in the beam transmission was overcome by the installation of a Large Bore Triplet (LBT) with six-inch aperture. In spite of the better transmission, beam simulation studies showed that the aberrations in the LBT were limiting the beam brightness [10]. As shown in [13], the intrinsic aberrations in electrostatic quadrupoles are of third order and the criteria for negligible emittance degradation can be written

$$\beta \ll f \sqrt{\frac{L}{\epsilon}}$$

β and ϵ are the transverse beta function and geometrical emittance of the beam respectively, L is the length of the quadrupole, and f is the focal length given by

$$f = \frac{V_{\text{ECR}} a^2}{VL}$$

with V_{ECR} the extraction voltage from the ECR and with a and V the radial aperture and voltage on the quadrupole electrodes. Using typical values, $f=0.5$ m, $L=10$ cm and $\epsilon=150 \pi \mu\text{m}$, one finds the criteria $\beta \ll 13$ m to avoid large aberrations. Using quadrupoles to focus ECR beams typically gives $\beta \gg 10$ m. Thus, aberrations in the quadrupoles can be large and limit the beam brightness which is consistent with results from beam simulations.

As mentioned in [13], increasing the length of the quadrupole reduces the aberrations. Since the aberrations are of third order, an octupole can also be used for active correction. Based on these two observations, a Double quadrupole Doublet with correcting octupole (DD) was designed and procured. The DD is currently installed under the RT ECR at the CCF as shown in Figure 1.

Eventually, another scheme was proposed to reuse the LBT. In this scheme, an Einzel Lens (EZ) was fabricated and installed between the ECR source and the LBT. The Einzel reduces the divergence of the beam and the beam size in the LBT and limits the brightness degradation in this device. The system EZ+LBT is currently installed under the SC ECR at the CCF as shown in Figure 1.

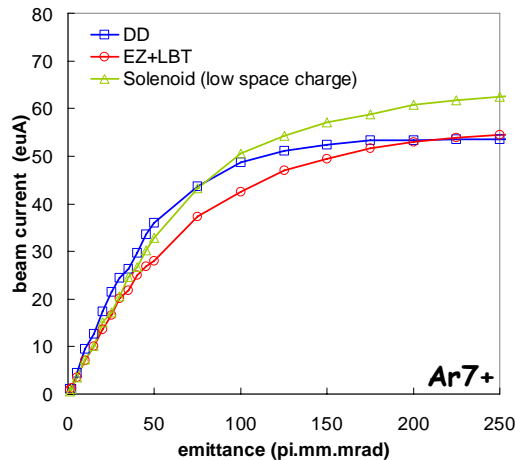


Figure 8: Beam brightness for the two electrostatic systems currently used under the production ECR sources at the CCF. The beam brightness for the solenoid system with low space charge effects is also given for comparison. All cases are for a 20 kV $^{40}\text{Ar}^{7+}$ beam from Artemis-B.

In Figure 8, the beam brightness for the DD and EZ+LBT systems are compared to the one for a solenoid with low space charge effects. Within the estimated 75 $\pi\cdot\mu\text{m}$ acceptance of the K500 cyclotron [14], the three systems are almost equivalent. Nonetheless, as mentioned above, the beam brightness using electrostatic systems is mildly affected by space charge effects whereas it can be significantly degraded when a solenoid is used.

In all cases of Figure 8, the focusing devices were tuned to obtain a waist in the analyzing magnet downstream. This tuning scheme was applied to avoid significant sextupole aberrations in the analyzing magnet. New magnets with a larger linear aperture have since been designed and procured.

NEW 90-DEGREE ANALYZING MAGNET

Beam dynamics studies on Artemis B have shown that the ECR beams have typically geometric transverse emittances around 200 $\pi\cdot\mu\text{m}$. For beams with such emittances, the field aberrations of the old 90-degree

analyzing magnet could significantly degrade the beam brightness. Limiting the beam size below 25 mm in the dipole by appropriately tuning the focusing elements above was done to mitigate the degradation of the beam brightness. Nonetheless, forcing a small beam size inside the dipole impacted the charge states selection because of the larger beam size at the collimating aperture. Thus, procuring new analyzing magnets with smaller field aberrations was pursued.

Table 1: Main parameters for the new analyzing magnets

Parameter	Value	Unit
Bending angle	90	degrees
Bending radius	40.6	cm
Gap	10	cm
Pole face angles	28.5	degrees
# of coils per magnet	2	-
# of turns per coil	36	-
Magnetic field	1.64	kG
Current	200	A
Voltage	16	V
Power	3.2	kW

The main design parameters for the new magnet are given in Table 1. The new 90-degree dipole is a room temperature H-type magnet that can transport a 200 $\pi\cdot\mu\text{m}$ beam without significant degradation of its brightness while still achieving good charge state separation.

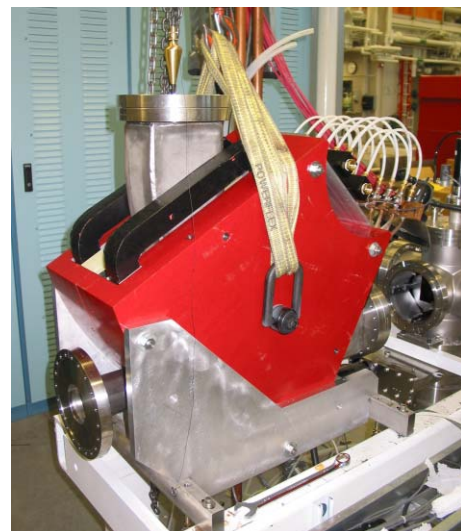


Figure 9: New analyzing magnet installed under Artemis-B in July 2007. The port on the left can be used for pumping.

The 2-D design was done with Poisson and the 3-D design with TOSCA. The fabrication is done in collaboration with the Texas A&M University Cyclotron Institute (TAMU-CI). Four new magnets are planned for

the NSCL and five for TAMU-CI. The magnet yokes and beam chambers are being fabricated at the NSCL while the coils were wound by TAMU-CI. Two new magnets have already been built and installed under Artemis and Artemis-B ECR ion sources at the NSCL. A picture of the new magnet during its installation on Artemis-B is shown in Figure 9. The quality control of the magnet was done using an identical beam test in the experiment and beam simulations. The simulations were done with KOBRA [15] using the 3D field maps calculated in TOSCA.

For the commissioning test, a $^{40}\text{Ar}^{7+}$ beam extracted at 20 kV is deflected horizontally and vertically using a steerer located one meter above the magnet and the beam centroid position is recorded on a beam viewer located 1.5 m after the magnet for each steerer setting. In the experiment, the magnetic steerer gave deflections of approximately 10 mrad/A. The simulated and measured response curves shown in Figure 10 are in good agreement proving that the magnet is performing according to design.

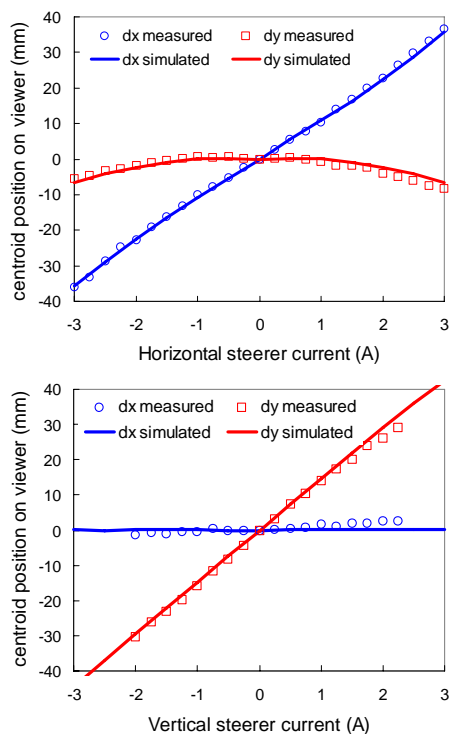


Figure 10: Simulated and experimental beam centroid response curves to horizontal (top) and vertical (bottom) deflection from a steerer located upstream of the new analyzing magnet. The centroid is measured on a beam viewer downstream of the analyzing magnet.

CONCLUSION

Significant increase in primary beam power has been achieved in the last three years at the CCF. A few beams have reached more than a kilowatt on production target and the improvements made in the injection beam line have largely contributed to the increase in performance.

Beam loss on the cyclotron deflectors and stripper foil lifetime are becoming two limiting factors to further increase the beam power. Ongoing R&D activities are trying to address these limitations.

REFERENCES

- [1] P.A. Závodszy et al., Nucl.Instr.Meth.B 241 (2005) 959
- [2] P.A. Závodszy et al., Rev. Sci. Instr. 77, 03A334 (2006)
- [3] P.A. Závodszy et al., "First Commissioning Results of the SuSI ECRIS" these proceedings
- [4] G. Machicoane et al., Rev. Sci. Instr. 77, 03A322 (2006).
- [5] M. Leitner, "Emittance Scanner Specification for the 88" Injector Beamlines" Technical Note, LBL
- [6] G. Machicoane et al., "R&D effort at NSCL with the off line ECR ion source Artemis-B," Proceedings of the 17th International Workshop on ECR Ion Sources, Lanzhou China, September 2006
- [7] M. Reiser, Theory and design of charged particle beams, Wiley series in beam physics, ISBN 0-471-30616-9
- [8] J.W. Stetson et al., "A Comparison of Electrostatic and Magnetic Focusing of Mixed Species Heavy Ion Beams at NSCL/MSU" Proceedings of PAC05, Knoxville, Tennessee, May 2005.
- [9] N. Kazarinov Rev. Sci. Instr. 75, 1665 (2004)
- [10] Q. Zhao et al., "Simulations of Solenoid and Electrostatic Quadrupole Focusing of High Intensity Beams from ECR Ion Source at NSCL," Proceedings of PAC05, Knoxville, Tennessee, May 2005.
- [11] G. Machicoane et al., "Experimental Evidences for Emittance Degradation by Space Charge Effects when using a focusing Solenoid below an ECR ion Source," Proceedings of ICIS2007, Jeju, South Korea, August 2007
- [12] F. Marti, NSCL internal note system
- [13] R. Baartman, "Aberrations in electrostatic quadrupoles" TRI-DN-95-21, TRIUMF, June 1995
- [14] S. L. Snyder, Study and Redesign of the NSCL K500 Injection, Central Region and Phase Selection Systems, Ph.D. Thesis, Michigan State University, 1995
- [15] P. Spaedtke, "KOBRA3-INP", 2005.